

Microscopic description of the pygmy and giant electric dipole resonances in stable Ca isotopes.

G.Tertychny^{a,b}, V.Tselyaev^{a,c}, S.Kamerdzhev^{a,b}, F.Grümmer^a, S.Krewald^a, J.Speth^a, A. Avdeenkov^{a,b}, E.Litvinova^b,

^a*Institut für Kernphysik, Forschungszentrum Jülich,
52425 Jülich, Germany*

^b*Institute of Physics and Power Engineering,
249020 Obninsk, Russia*

^c*Institute of Physics S.Petersburg University, Russia
(Dated:)*

The properties of the pygmy (PDR) and giant dipole resonance (GDR) in the stable ^{40}Ca , ^{44}Ca and ^{48}Ca isotopes have been calculated within the *Extended Theory of Finite Fermi Systems* (ETFFS). This approach is based on the random phase approximation (RPA) and includes the single particle continuum as well as the coupling to low-lying collective states which are considered in a consistent microscopic way. For ^{44}Ca we also include pairing correlations. We obtain good agreement with the experimental data for the gross properties of both resonances. It is demonstrated that the recently measured A-dependence of the strength of the PDR below 10 MeV is well understood in our model: due to the phonon coupling some of the strength in ^{48}Ca is simply shifted beyond 10 MeV. The predicted fragmentation of the PDR can be investigated in (e, e') and (γ, γ') experiments. Whereas the isovector dipole strength of the PDR is small in all Ca isotopes, we find in this region surprisingly strong isoscalar dipole states, in agreement with an $(\alpha, \alpha'\gamma)$ experiment. We conclude that for the detailed understanding of the structure of excited nuclei e.g. the PDR and GDR an approach like the present one is absolutely necessary.

PACS: 24.30.Cz; 21.60.Ev; 27.40.+z

Keywords: Microscopic theory, Pygmy and giant dipole resonances, Single-particle continuum, Transition densities.

I. INTRODUCTION

The pygmy dipole resonance (PDR) or "soft" electric dipole resonances have attracted the interest of several research groups in the past decade [1, 2]. The PDR is defined as a part of the low-energy tail of the isovector dipole resonance (GDR) and dwells well below the GDR maximum. In phenomenological models these resonances are described as vibrations of the excess neutrons (neutron skin) against an inert core with $N=Z$ [3]. Therefore, one expects little strength in $N=Z$ nuclei and increasing strength with increasing neutron excess. In exotic nuclei with extreme neutron excess these PDR should be especially pronounced. As the dipole strength near the nucleon separation energy strongly influences the r-process in astrophysics, the PDR in such nuclei is of importance for the nuclear synthesis.

Another important reason of the interest in the PDR are modern experimental techniques which allow to distinguish between $1^-, 2^+$ and 1^+ states [2, 4]. In recent experiments new data have been obtained for several groups of isotopes (see [1, 5, 6]) including the stable Ca isotopes [5, 6]. The latter results for the three nuclei ^{40}Ca , ^{44}Ca and ^{48}Ca , which are the bridge between light and medium weight nuclei, are especially interesting. The experiment shows a large difference in the summed E1 strengths of the PDR below 10 MeV for ^{40}Ca

and ^{44}Ca . Surprisingly the EWSR of the PDR does not rise with the neutron excess but is roughly the same for ^{44}Ca and ^{48}Ca . This contradicts the phenomenological models as well as microscopic RPA calculations [7].

Clearly, such an analysis should be performed within microscopic theoretical approaches which simultaneously describes the PDR and GDR and other nuclear structure properties. The models should not have free fitting parameters for each nucleus in order to obtain reliable results which allow to understand the underlying physics. Such an analysis has been performed in ref. [7] for the three Ca isotopes within the RPA based on the self-consistent density functional method and for heavier nuclei within the relativistic self-consistent RPA or QRPA based on the relativistic Hartree-Bogoliubov model [8]. In both approaches the self-consistency ensured a reliable comparison between different nuclei. Goriely and Khan [9] calculated within the self-consistent QRPA the E1 strength distributions [9] for all nuclei with $8 \leq Z \leq 110$ between the proton and neutron drip lines using known Skyrme forces. In their calculation the low-lying E1 strength was located systematically higher by some 3 MeV compared with the available data.

In the past 15 years Kamerdzhev, Speth, Tertychny and Tselyaev have developed the *Extended Theory of Finite Fermi Systems* (ETFFS) which uses the Green function formalism, is based on the RPA and includes the single-particle continuum as well as the coupling to the low-lying phonons. It also considers the effect of the phonons in the ground state correlations. The authors have shown in numerous publications (see [10] and references therein), that this approach allows to calculate simultaneously low-lying as well as high lying nuclear

structure properties in quantitative agreement with the experimental data. The model has been applied to all closed shell nuclei. As far as the electric dipole states are concerned the complete spectrum has always been calculated, but as the PDR are weak compared to the GDR they appear only as small fluctuations at the lower end of the GDR.

The first calculations of the PDR within this model including pairing have been performed for Ca [6] and Sn [11] isotopes. Here the characteristics of the PDR are in much better agreement with the data than the above mentioned self consistent calculations. This is due to coupling to the phonons, first of all, and due to another single-particle scheme. There exists a basic difference between the present approach and self-consistent (Q)RPA calculations e.g. [7, 8, 9] as we will discuss below.

Long time ago the conventional (1p-1h) RPA and QRPA have been extended to include the effects of phonons. Soloviev et al. introduced 30 years ago the *Quasiparticle Phonon Model (QPM)* [12, 13], the present model (*ETFFS*) was first applied nearly 15 years ago in ref. [14, 15] and around the same time Broglia et al. developed the *Phonon Coupling Model (PCM)* [16]. However, the extended models [10, 16] have been used only recently to calculate the properties of PDR in non-magic nuclei because an additional work had to be done to include pairing to these models. In addition to the above mentioned results, the PDR calculations have been performed for ^{208}Pb [17] and for a long Sn isotopes chain [18] within the QPM, for ^{120}Sn , ^{132}Sn , ^{208}Pb (together with the giant E1 resonances) [19] and for ^{18}O , ^{20}O , ^{22}O [20] within the PCM generalized to include pairing. Very recently, the E1 photo absorption cross sections have been calculated in ^{116}Sn , ^{120}Sn and ^{124}Sn with a version of the ETFFS (see below) [21], which also considers pairing. So far the single-particle continuum for non-magic nuclei has been only taken into account in the present approach (ETFFS) [6, 11, 21].

In the recent *ETFFS* calculations for the PDR in Ca isotopes [6], several approximations (for details see [11]) have been made which were responsible that the theoretical results agreed only qualitatively with the data. The aim of the present investigation is threefold: firstly, we repeat the previous calculations without the approximations and apply for ^{44}Ca the generalized version of the *ETFFS* which includes the pairing effects, secondly we clarify the role of the continuum for PDR and GDR, which has attracted a great interest now [22], and finally we investigate in detail the microscopic structure of the PDR, especially the role of the isoscalar dipole components. The result of the present calculation agrees well with the experimental data [5, 6] and it explains in a natural way the somewhat surprising result that the strength of the PDR does (seemingly) not scale with the neutron excess.

II. METHOD

We have used the generalized version of the ETFFS with pairing which differs from the one used in [6, 11] by taking into account the self-energy and the induced ph- and pp- interaction graphs on the same footing, i.e. by a consistent summations of the so-called g^2 diagrams where g is the amplitude for low-lying phonon creation. The formalism developed for nuclei with pairing, is called *Quasiparticle Time Blocking Approximation (QTBA)*, and is described in detail in [23] and [21]. (However, the ground state correlations induced by the phonon coupling have not been included to the present calculations). The single-particle continuum has been included on the RPA level where it is taken into account correctly within our Green function technique in the coordinate representation. For details see [10]. Therefore in our approach we consider the three mechanisms which create the width of giant resonance, namely (I) the Landau damping ((Q)RPA configurations), (II) the escape width (the single-particle continuum) and (III) the spreading width (phonon coupling, or complex configurations). As in all our previous calculations within the ETFFS, we include the most collective low-lying phonons, namely 3_1^- , 5_1^- phonons for ^{40}Ca , and 2_1^+ , 3_1^- , 5_1^- phonons for ^{44}Ca and ^{48}Ca . The collective phonons have been microscopically calculated within the RPA for ^{40}Ca and ^{48}Ca . In the case of ^{44}Ca we used the corresponding QRPA with pairing. The standard BCS equation have been applied using the particle-particle Landau-Migdal forces [24]. In the present and in our previous calculations we used the special "forced consistency" procedure [25] to obtain the energy of the spurious E1 state to be exactly equal to zero without the procedure of fitting force parameters.

As in our previous calculations we used the effective particle-hole Landau-Migdal interaction:

$$F(\mathbf{r}, \mathbf{r}') = C_0[f(r) + f'(r)\boldsymbol{\tau}_1 \cdot \boldsymbol{\tau}_2 + (g + g'\boldsymbol{\tau}_1 \cdot \boldsymbol{\tau}_2)\boldsymbol{\sigma}_1 \cdot \boldsymbol{\sigma}_2] \delta(\mathbf{r} - \mathbf{r}'), \quad (2.1)$$

with the conventional interpolation formula, for example, for the parameter f

$$f(r) = f_{ex} + (f_{in} - f_{ex})\rho_0(r)/\rho_0(0) \quad (2.2)$$

and similarly for the other r -dependent parameters. Here $\rho_0(r)$ is the density distribution of the ground state of the nucleus under consideration and f_{in} and f_{ex} are the force parameters inside and outside of the nucleus. The standard values of the parameters, which have been already used for all the nuclei under consideration [6, 10, 11], are as follows

$$f_{in} = -0.002, \quad f_{ex} = -1.4, \quad f'_{ex} = 2.30, \quad f'_{in} = 0.76,$$

$$g = 0.05, \quad g' = 0.96, \quad C_0 = 300 \text{ MeVfm}^3. \quad (2.3)$$

For the nuclear density $\rho_0(r)$ in the interpolation formula we chose the theoretical ground state density distribution

of the corresponding nucleus,

$$\rho_0(r) = \sum_{\epsilon_i \leq \epsilon_F} \frac{1}{4\pi} (2j_i + 1) R_i^2(r), \quad (2.4)$$

which is more consistent than the previously used Woods-Saxon distribution. For that reason we had to readjust f_{ex} and obtained the value of $f_{ex} = -1.4$ used [26]. Here $R_i(r)$ are the single-particle radial wave functions of the single-particle model used. For other details of the calculations, see [6, 10, 11].

III. PDR RESULTS

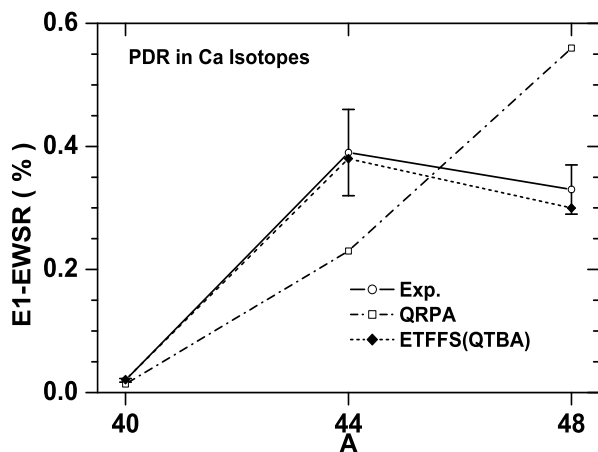


FIG. 1: The energy-weighted electric dipole strength integrated up to 10 MeV is shown for the isotopes ^{40}Ca , ^{44}Ca , and ^{48}Ca . Dashed: experimental data taken from [6]; dash-dotted: quasiparticle random phase approximation, full: extended theory of finite Fermi systems in the quasiparticle time blocking approximation (including pairing for ^{44}Ca)

The main results of our calculations for the gross properties PDR are given in Fig.1 and Table I. Within the experimental errors, our theoretical results agree with the data as shown in *Table I*. This holds for the total $B(E1)$ strength, EWSR and the EWSR share in the energy interval up to 10 MeV. As for the PDR mean energies, which were defined as $\bar{E} = \Sigma E_i B_i(E1) / \Sigma B_i(E1)$, the agreement is rather good for ^{44}Ca and ^{48}Ca but the theoretical result 8.68 MeV is too high in ^{40}Ca . In all the cases the results of the extended theory, i.e. inclusion of phonon coupling and single-particle continuum, give rise to a considerable improvement compared to the (Q)RPA results. and (especially for ^{44}Ca) our results of ref. [6]. The latter is due to an improvement of the theory but even more importantly to more careful calculations of the single-particle levels and of the (Q)RPA phonons, including the use of eq.(2.4) for them.

In Fig.1 we compare the theoretical EWSR of ^{40}Ca , ^{44}Ca and ^{48}Ca for the isovector dipole strength up to 10 MeV with the experimental data. The dash-dotted line is the (Q)RPA result which rises with neutron excess in agreement with the phenomenological model. The experiment shows only a strong increase for ^{44}Ca compared to ^{40}Ca but the strength of ^{48}Ca and ^{44}Ca does not change within the experimental errors. The ETFFS result reproduces this somewhat surprising result.

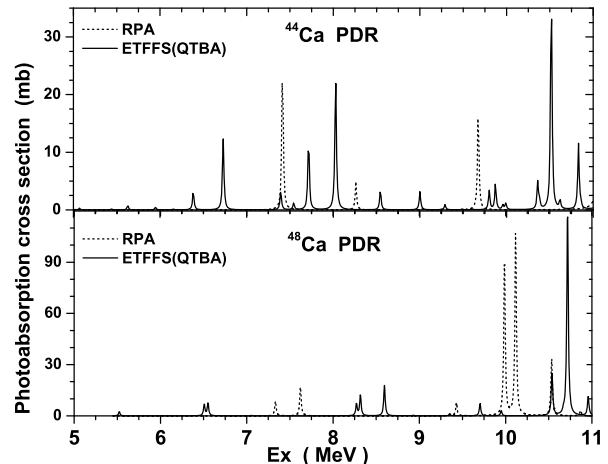


FIG. 2: Pygmy resonances in ^{44}Ca and ^{48}Ca up to 11 MeV

The explanation is given in Fig.2 where we compare the theoretical PDR-spectrum of ^{44}Ca and ^{48}Ca . Whereas the (Q)RPA result is in both cases around 10 MeV and below, the ETFFS result differs in the two nuclei. Due to the phonon splitting an appreciable fraction of the strength in ^{48}Ca is shifted to about 11 MeV and has therefore not be measured in the cited experiment. If one adds this part (the 10 MeV limit is somewhat arbitrary) the total PDR strength increase also in ETFFS with the neutron excess. One also realizes that the PDR for the open shell nucleus ^{44}Ca is somewhat lower compared to the PDR in the closed shell nucleus ^{48}Ca .

In Fig.3 the transition densities for protons and neutrons of the electric dipole isovector strength up to 10 MeV are shown for the three Ca isotopes. In ^{40}Ca the density is of purely isoscalar nature. With increasing neutron excess the neutron density is slightly shifted to a larger radius, indicating some an isovector admixture, but the isoscalar character remains. This is easily understood in the framework of microscopic models. The isovector ph-interaction is repulsive and shifts the low-lying isovector strength into the region of the GDR. On the other hand, the isoscalar ph-interaction is attractive and shifts some of the high lying isoscalar dipole strength to lower energies and gives rise to some isoscalar collectivity below 10 MeV in contrast to the isovector case.

In Fig.4 the isoscalar strength distributions (with the

TABLE I: Properties of the pygmy dipole resonances in Ca isotopes in the (5 - 10) MeV interval. (The experimental data taken from [6])

		^{40}Ca	^{44}Ca	^{48}Ca
$\sum_i B_i(E1)\uparrow$, $10^3 e^2 \text{fm}^2$	(Q)RPA	2.51	45.6	97.4
	ETFFS(QTBA)	3.67	81.0	66.2
	Exp.	5.1 ± 0.8	92.2 ± 15.6	68.7 ± 7.5
$\sum_i E_i B_i(E1)\uparrow$, $\text{keV} e^2 \text{fm}^2$	(Q)RPA	21.48	374.9	897.3
	ETFFS(QTBA)	31.86	611.0	527.7
	Exp.	35 ± 5	629 ± 107	570 ± 62
$\sum_i E_i B_i(E1)\uparrow$, % EWSR	(Q)RPA	0.014	0.23	0.56
	ETFFS(QTBA)	0.021	0.38	0.30
	Exp.	0.020 ± 0.003	0.39 ± 0.07	0.33 ± 0.04
\bar{E} , MeV	(Q)RPA	8.84	8.22	9.30
	ETFFS(QTBA)	8.68	7.54	7.97
	Exp.	6.80	7.10	8.40

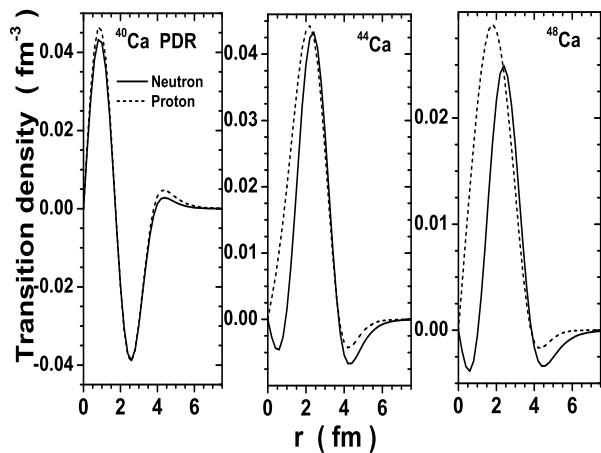


FIG. 3: Transition densities of the electric dipole strength in the (5-10)MeV interval

operator $\mathbf{r}^3 Y_{10}$) in ^{40}Ca and ^{48}Ca calculated within the ETFFS and RPA are shown. In ^{40}Ca the influence of the phonons are small compared to ^{48}Ca especially for the low energy spectrum. Whereas in ^{40}Ca the phonons only give rise to an energy shift one observes in ^{48}Ca also some fragmentation of the low lying strength. This fragmentation is due to the low-lying 2^+ state which can be coupled to $1p1h$ 1^- states to produce the necessary 1^- complex configurations. The corresponding states do not exist in ^{40}Ca . The two peaks in ^{40}Ca at 5.8 MeV and 7.8 MeV are in an agreement with the experimental finding [27].

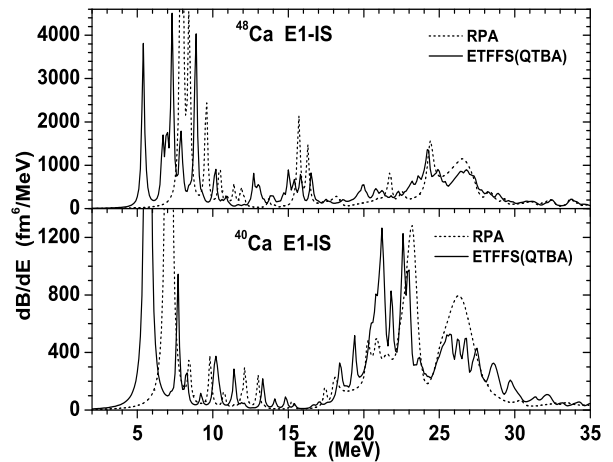


FIG. 4: Isoscalar electric dipole strength in Ca^{40} and Ca^{48}

IV. THE GIANT RESONANCE RESULTS

For consistency we also calculated the giant isovector resonances in the three calcium isotopes. Results are presented in Table II and in Figs.5 and 6. In Table 2 the results obtained in three different approximations are shown: (Q)RPA calculations with the single-particle continuum as well as the ETFFS(QTBA) calculations with and without the continuum. The theoretical values are extracted from the calculated strength distribution under the condition that the three lowest energy-weighted moments of the Lorentzian and the theoretical curve should coincide in the (10-40) MeV interval [14, 28]. The averaging parameter Δ which was used in addition to the single-particle continuum the giant resonance calculation was 400 keV. The differences between the (Q)RPA and

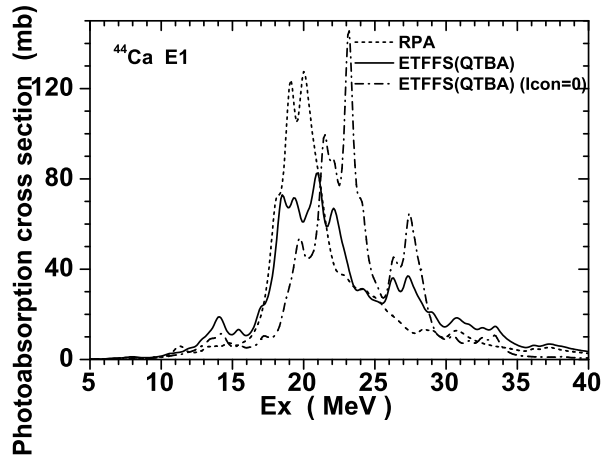


FIG. 5: Giant electric dipole resonance in ^{44}Ca calculated in three different approximations: (I) ETFFS(QTBA) (full line), (II) QRPA (dash-dotted); (III) ETFFS(QTBA) without continuum (dash-dotted)

TABLE II: Properties of the isovector giant dipole resonances in Ca isotopes

		^{40}Ca	^{44}Ca	^{48}Ca
% EWSR	(Q)RPA	102.3	106.6	91.2
	ETFFS(QTBA)-c*	100.4	108.6	91.4
	ETFFS(QTA)B	103.7	110.5	93.0
	Exp.	106.3		119.5
\bar{E} , MeV	(Q)RPA	21.0	20.4	16.8
	ETFFS(QTBA)-c	22.7	23.1	19.9
	ETFFS(QTBA)	20.9	21.2	18.4
	Exp.	20.0		19.6
σ_{\max} , mb	(Q)RPA	137.2	146.6	170.6
	ETFFS(QTBA)-c	137.2	129.2	113.7
	ETFFS(QTBA)	75.6	80.9	85.4
	Exp.	95.0		102.7
Γ , MeV	(Q)RPA	2.9	3.2	2.6
	ETFFS(QTBA)-c	3.2	3.8	4.1
	ETFFS(QTBA)	6.2	6.4	5.7
	Exp.	5.0		7.1

* -c stands for calculations without continuum.

full ETFFS(QTBA) are most striking for the width Γ and the maximum of the photo absorption cross section σ_{\max} , where the results differ nearly by a factor of two. We obtain good agreement with the experiments only within our full model, i.e. including the phonons and the single-particle continuum. Here we want to stress that we calculate GDR and the low-lying states simultaneously within the same configuration space and with the same forces.

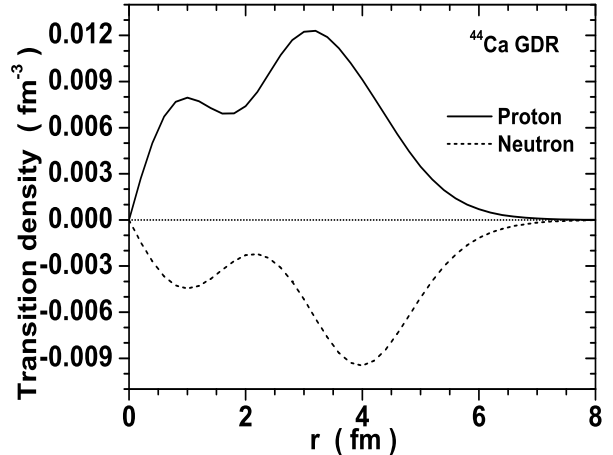


FIG. 6: Transition densities for ^{44}Ca ; the isovector electric dipole strength is integrated in the (15-30) MeV interval

As compared with our earlier results for ^{40}Ca and ^{48}Ca [14, 26], here the ground state correlations induced by the phonon coupling were not taken into account and we have chosen a different energy interval for the summation. In addition, a different definition for the mean energy and another "refining" procedure [23] have been used. Like in the previous calculations of giant multipole resonances in closed shell nuclei [10] the inclusion of phonon coupling, i.e. the calculation within the full ETFFS (QTBA), increases the widths by a factor of 2 and (except for ^{40}Ca) shifts the mean energies by 1.0-1.5 MeV to higher energy.

In Fig.5 the results for the GDR in ^{44}Ca are shown, calculated again within the three approximations. In the full model an appreciable fraction of the strength is shifted to much higher energies compared to the QRPA result which give rise to an asymmetric shape. Finally in Fig.6 the transition density for the GDR in ^{44}Ca is plotted. It has the expected isovector shape.

In order to study the role of the single-particle continuum we have calculated the giant resonance (see Table 2 and Fig.5) and PDR characteristics without the continuum. It should be expected that the role of the single-particle continuum is important in light nuclei. It is of special interest to consider the question within the same calculational scheme for the Ca isotopes, including the non-magic ^{44}Ca , because there is no information about the role of the continuum in the approaches of similar kind in non-magic nuclei. One can see from Table 2 and Fig.5 a very noticeable influence of the continuum for the integral characteristics in all the Ca isotopes as well as for the strength distribution. Moreover, the continuum's influence is noticeable even for the PDR: our full calculations have given 0.38% of the EWSR in the (5.0-10.0) MeV interval for ^{44}Ca whereas the calculation without continuum gave 0.19%. The exclusion of the continuum also results in a considerable redistribution of the PDR

strength. These features can be studied in experiments with electrons and gamma-rays.

V. SUMMARY

We have investigated the low-lying (PDR) and high-lying (GDR) electric dipole states in the magic ^{40}Ca and ^{48}Ca and non-magic ^{44}Ca within the ETFFS(QTBA) which, in addition to the standard (Q)RPA, takes into account the single-particle continuum and phonon coupling. In the present approach we corrected for the double counting due to the phonons in our generalized propagator. Good agreement with experiment available for integral characteristics has been found.

The agreement for the PDR is much better as compared with the previous ETFFS calculations [6]. The PDR, i.e. the isovector dipole strength below 10 MeV, is less than 1 percent of the energy weighted sum rule because the strongly repulsive isovector force shift the strength into GDR region. In order to investigate the structure of the PDR further we calculated the corresponding transition densities. It turned out that these densities are isoscalar with some isovector admixture in ^{44}Ca and ^{48}Ca which is due to the strongly attractive isoscalar interaction which shifts the high-lying isoscalar strength below 10 MeV.

In ^{40}Ca we obtain two prominent isoscalar dipole states (induced by the external field $\mathbf{r}^3 Y_{10}$) at 5.8 MeV and 7.8 MeV. The predicted isoscalar strength can be detected in $(\alpha, \alpha'\gamma)$ experiments, see [29].

We have shown that the role of the single-particle continuum is very noticeable for the GDR and quantitatively important for the PDR in the Ca isotopes considered. The same should be true for lighter nuclei too. Thus, taking into account the new effects as compared with the standard RPA or QRPA, i.e. the phonon coupling and single-particle continuum, is necessary to explain the properties of both these resonances.

VI. ACKNOWLEDGMENTS

The authors are very thankful to N. Luytorovich for permanent collaboration in the preparation of this article and to A.Zilges for the information about the experiments [29]. S.Kamerdzhev thanks the Institute for Nuclear Theory (Seattle, USA) for partial support during the participation in the Program INT-05-3 which was very useful for this work. The work was supported in part by the DFG and RFBR grants Nos.GZ:432RUS113/806/0-1 and 05-02-04005 and by the INTAS grant No.03-54-6545.

-
- [1] R. Palit, P. Adrich, T. Aumann, et al., Nucl. Phys. A731 (2004) 235.
 - [2] U. Kneisl, H.H. Pilz, and A. Zilges, Progr. Part. Nucl. Phys. 37 (1996) 349.
 - [3] Y. Suzuki, K. Ikeda, and H. Sato, Progr. Theor. Phys. 83 (1990) 180.
 - [4] R.M.Laszewski, P.Rullhusen, S.D.Hoblit and S.F.LeBrun, Phys. Rev. Lett. 54 (1985) 530.
 - [5] T. Hartmann, J. Enders, P.Mohr, et al., Phys. Rev. C 65 (2002) 034301.
 - [6] T. Hartmann, M. Babilon, S. Kamerdzhev, et al., Phys. Rev. Lett. 93 (2004) 192501.
 - [7] J. Chambers, E. Zaremba, J.P. Adams, and B.Castel, Phys. Rev. C 50 (1994) 2671R.
 - [8] D. Vretenar, A.V. Afanasjev, G.A. Lalazissis, and P.Ring, Phys. Rep. 409 (2005) 101.
 - [9] S. Goriely, E. Khan, Nucl.Phys. A 706 (2002) 217.
 - [10] S. Kamerdzhev, J. Speth, G. Tertychny, Phys. Rep. 393 (2004) 1.
 - [11] S.P. Kamerdzhev and E.V. Litvinova, Phys. At. Nucl. 67 (2004) 183; erratum Phys. At. Nucl. 67 (2004) 1610.
 - [12] V.G. Soloviev, Theory of Complex Nuclei (Pergamon Press, Oxford, 1976) [Russ. original, Nauka, 1971]
 - [13] V.G. Soloviev, Theory of Atomic Nuclei: Quasiparticles and Phonons (Institute of Physics, Bristol and Philadelphia, USA, 1992)
 - [14] S. Kamerdzhev, J. Speth, G. Tertychny and V.Tselyaev, Nucl.Phys. A555 (1993) 90.
 - [15] S. Kamerdzhev, J. Speth, G. Tertychny and J.Wambach,Z.Physik A 336 (1993) 253.
 - [16] G. Colo, Nguyen Van Giai, P.F. Bortignon, R.A Broglia, Phys. Rev. C 50 (1994) 1496.
 - [17] N. Ryezaeva, T. Hartmann, Y. Kalmykov, et.al., Phys. Rev. Lett. 89 (2002) 272502.
 - [18] N. Tsoneva, H. Lenske, Ch. Stoyanov, Phys. Lett. B 586 (2004) 213.
 - [19] D.Sarchi, P.F. Bortignon, G. Colo, Phys. Lett. B 601 (2004) 27.
 - [20] G. Colo, P.F. Bortignon, Nucl.Phys.A 696 (2001) 427.
 - [21] E.V. Litvinova, V.I. Tselyaev, arXiv:nucl-th/0512030 v2 9 Dec 2005.
 - [22] A. Richter, Progr. Part. Nucl.Phys. 55 (2005) 387.
 - [23] V.I. Tselyaev arXiv:nucl-th/0505031 v1 May 2005
 - [24] M.V. Zverev, E.E. Saperstein, Yad.Fiz. 42 (1982) 1985.
 - [25] S.Kamerdzhev,R.J.Liotta,E.Litvinova and V.Tselyaev, Phys.Rev.C 58 (1998) 172
 - [26] S. Kamerdzhev, J. Speth, G. Tertychny, Nucl.Phys. A 624 (1997) 328.
 - [27] M.N. Harakeh and A.van der Woude, Giant Resonances (Clarendon Press, Oxford, 2001).
 - [28] V.I. Tselyaev, Bull. Rus. Acad. Sci. Phys. 64 (2000) 434.
 - [29] A. Zilges, M. Babilon, T.Hartmann, et al.,Progr. Part. Nucl. Phys. 55 (2005) 408.